Enantioselectivity in the Regioirregular Placements and Regiospecificity in the Isospecific Polymerization of Propene with Homogeneous Ziegler-Natta Catalysts

Gaetano Guerra,* Luigi Cavallo, Gilberto Moscardi, Michele Vacatello, and Paolo Corradini

Contribution from the Dipartimento di Chimica, Università di Napoli, Via Mezzocannone 4, I-80134, Napoli, Italy

*Received June 30, 1993. Revised Manuscript Received December 10, 1993**

Abstract: With the aim of a possible rationalization of the probability distributions of stereochemical configurations of the regioirregular units in isotactic polymer samples (prepared in the presence of *rac*-ethylenebis(4,5,6,7-tetrahydro-1-indenyl)zirconium dichloride or *rac*-ethylenebis(1-indenyl)zirconium dichloride and methylaluminoxane), a detailed molecular mechanics analysis on previously proposed model catalytic sites is reported. In particular, catalytic intermediates suitable for primary and secondary insertions of propene on primary and secondary polypropene chains, for both systems with *rac*-ethylenebis(4,5,6,7-tetrahydro-1-indenyl) and *rac*-ethylenebis(1-indenyl) ligands, are compared. The models are able to rationalize the observed enantioselectivities, not only for the regioregular placements but also for the regioirregular placements (secondary insertion on a primary chain and primary insertion on a secondary chain). Moreover, the nonbonded interactions in the models give a contribution in favor of the monomer coordination suitable for the primary insertion, even after an occasional secondary insertion, and are able to account for the higher regiospecificity observed for titanocene-based, with respect to zirconocene-based, catalytic systems.

Introduction

The application of simple molecular mechanics techniques to possible model catalytic sites for the heterogeneous[1-5] and homogeneous[6-9] Ziegler-Natta polymerizations has allowed not only to rationalize several experimental facts but also to make correct predictions of the stereospecificity of some new catalytic complexes.

In particular, the main contribution of molecular mechanics calculations to the comprehension of the behavior of Ziegler-Natta catalysts has been, in our opinion, the discovery that the mechanism of enantioselectivity involves a "chiral orientation of the growing chain",[1,6,8,10] which had been never considered before, even only as possible in principle.

Another interesting result of the nonbonded energy analyses, common to the considered metallocene models, is that the regiospecificity of polymerization (primary insertion of the propene is favored)[11-13] is qualitatively accounted for by steric interactions in the model intermediates corresponding to the monomer coordination step, without considering possible electronic factors. In fact, the orientation of a coordinated propene monomer suitable for secondary insertion, that is, the one showing the monomer methyl substituent on the opposite side with respect to the growing chain, was found to be, in our models, energetically disfavored with respect to the orientation suitable for primary insertion.[6,7,9]

Analogous results have been obtained in a recent combined *ab-initio* and molecular mechanics study,[14] in which the regioselectivity in propene polymerization is explained on the sole basis of the molecular mechanics interactions active in the transition state of the insertion step. It is interesting to note that the transition state, as obtained by *ab-initio* methods in ref 14, shows Zr-C (olefin) distances similar to those assumed in our models of catalytic intermediates. The same authors report an opposite regioselectivity for a calculated π-complex which they assume is the intermediate corresponding to the monomer coordination step. This is due, in our opinion, to the large, and possibly unrealistic, values of the Zr-C (olefin) distances obtained for these π-complexes by *ab-initio* calculations (2.90 and 2.97 Å). For instance, the latter distances are much higher than those observed in the crystalline structures of the Zr complex $Cp_2Zr(C_2H_4)(PMe_3)$[15] (2.36 Å), of the Ti complex $Cp_2Ti(C_2H_4)$[16] (2.16 Å), and of the Nb complex $Cp_2Nb(C_2H_4)C_2H_5$[17] (2.19 Å) (showing a σ-coordinated alkyl group and a π-coordinated olefin, as in the model catalytic intermediates). A relatively recent collection of data[18] reports Mt-C (olefin) distances in the range 1.99-2.54 Å, changing the metal and the other ligands. However, for a given metal the standard deviation (considering complexes with different ligands, coordination numbers, and oxidation states) is generally lower than 0.1 Å.[18] Long, but asymmetric, Zr-C (olefin) distances (2.90 and 2.40 Å) have been also calculated for an analogous

* Abstract published in *Advance ACS Abstracts*, February 1, 1994.

(1) Corradini, P.; Barone, V.; Fusco, R.; Guerra, G. *Eur. Polym. J.* **1979**, *15*, 133.
(2) Corradini, P.; Barone, V.; Fusco, R.; Guerra, G. *J. Catal.* **1982**, *77*, 32.
(3) Corradini, P.; Barone, V.; Guerra, G. *Macromolecules* **1982**, *15*, 1242.
(4) Corradini, P.; Barone, V.; Fusco, R.; Guerra, G. *Gazz. Chim. Ital.* **1983**, *113*, 601.
(5) Corradini, P.; Guerra, G.; Villani, V. *Macromolecules* **1985**, *18*, 1401.
(6) Corradini, P.; Guerra, G.; Vacatello, M.; Villani, V. *Gazz. Chim. Ital.* **1988**, *118*, 173.
(7) Cavallo, L.; Corradini, P.; Guerra, G.; Vacatello, M. *Macromolecules* **1991**, *24*, 1784.
(8) Venditto, V.; Guerra, G.; Corradini, P.; Fusco, R. *Polymer* **1990**, *31*, 530.
(9) Cavallo, L.; Corradini, P.; Guerra, G.; Vacatello, M. *Polymer* **1991**, *32*, 1329.
(10) Corradini, P.; Guerra, G. *Prog. Polym. Sci.* **1991**, *16*, 239.
(11) Ewen, J. A. *J. Am. Chem. Soc.* **1984**, *106*, 6355.
(12) Longo, P.; Grassi, A.; Pellecchia, C.; Zambelli, A. *Macromolecules* **1987**, *20*, 1015.
(13) Ewen, J. A.; Elder, M. J.; Jones, R. L.; Haspeslagh, L.; Atwood, J. L.; Batt, S. G.; Robinson, K. *Makromol. Chem. Symp.* **1991**, *48/49*, 253.
(14) Kawamura-Kuribayashi, H.; Koga, N.; Morokuma, K. *J. Am. Chem. Soc.* **1992**, *116*, 8687.
(15) Alt, G. H.; Denner, C. E.; Thewalt, U.; Rausch, M. D. *J. Organomet. Chem.* **1988**, *356*, C83.
(16) Cohen, S. A.; Auburn, P. R.; Bercaw, J. E. *J. Am. Chem. Soc.* **1983**, *105*, 1136.
(17) Guggenberg, L. J.; Meakin, P.; Tebbe, F. N. *J. Am. Chem. Soc.* **1974**, *96*, 5420.
(18) Orpen, A. G.; Brammer, L.; Allen, F. H.; Kennard, O.; Watson, D. G.; Taylor, R. *J. Chem. Soc., Dalton Trans.* **1989**, *S1*.

0002-7863/94/1516-2988$04.50/0

intermediate by other recent *ab-initio* calculations.[19] However, shorter and symmetric Zr–C (olefin) distances (2.5 Å) have been adopted in the latter study for the activated complex used in the subsequent molecular mechanics calculations.

Our previous molecular mechanics calculations have also shown that primary insertions and (infrequent) secondary insertions tend to occur with the opposite enantioface of the monomer in isospecific model sites (Figure 4 in ref 6).

Recently, a complete determination of the stereochemical configuration of the regioirregular units in the isotactic polymer (prepared in the presence of *rac*-ethylenebis(4,5,6,7-tetrahydro-1-indenyl)zirconium dichloride[20–22] or *rac*-ethylenebis(1-indenyl)-zirconium dichloride[20,21,23,24] and methylaluminoxane) has been obtained by NMR characterizations. In particular, it has been clearly established that (i) the primary (largely prevailing) and secondary insertions of propene on a primary growing chain (that is, a growing chain in which the last inserted unit was obtained by a primary insertion of propene) occur preferably with opposite enantiofaces;[20,23] (ii) the primary insertion of propene is favored with respect to the secondary insertion also in the presence of a secondary growing chain (one in which the last inserted unit was obtained by a secondary insertion of propene);[20,21,23,24] that is, only isolated secondary propene units are observed; and (iii) the primary insertion of propene occurs with preference for a given enantioface, irrespective of the primary or secondary nature of the growing chain. However, the enantioselectivity for the primary insertion on a secondary growing chain is high for the catalytic system with the *rac*-ethylenebis(4,5,6,7-tetrahydro-1-indenyl) ligand and low for the catalytic system with the *rac*-ethylenebis-(1-indenyl) ligand.[20,21,23]

With the aim of a possible rationalization of these observed behaviors, we report in this paper the results of a detailed analysis of the previously proposed model catalytic sites for the homogeneous isospecific polymerization of propene. In particular, we compare catalytic intermediates (corresponding to the coordination step) suitable for primary and secondary insertions of propene on primary and secondary polymeryl groups in the two systems with *rac*-ethylenebis(4,5,6,7-tetrahydro-1-indenyl) and *rac*-ethylenebis(1-indenyl) ligands.

The calculations performed were aimed, as in our previous studies, at (i) recognizing the "stable" geometries of the relevant diastereoisomers; (ii) choosing, among these, the geometries which are as near as possible to the transition state; and (iii) making comparative estimates of the corresponding activation energies.

At variance with previous calculations, the coordinates of the atoms in the various conformations of the model systems considered in this paper have been obtained relaxing most of the internal coordinates. As a result, the internal energies calculated away from the minima are lower and more realistic than those reported in our previous papers. We want to stress that no significant changes in the main reported results are obtained by the present more realistic calculations, as we already anticipated.

In addition, although we believe that the Zr–C (olefin) distance in the coordination intermediates should be in the range 2.3–2.5 Å (see next section), since much larger values have been calculated by the previously cited *ab-initio* studies,[14,18] the dependence of our results on this distance (in the very broad range 2.2–2.8 Å) has been also explored.

Models and Methods

The basic models of the catalytic sites considered in this paper are metal complexes containing three ligands, that is, a π-coordinated propene molecule, a σ-coordinated isobutyl or *sec*-butyl group (simulating a primary or a secondary growing chain, respectively), and a chelating *rac*-ethylenebis(4,5,6,7-tetrahydro-1-indenyl) or *rac*-ethylenebis(1-indenyl) ligand (in the following referred to as en(thind)$_2$ and en(ind)$_2$, respectively).

A prochiral olefin such as propene may give rise to nonsuperposable coordinations, which can be labeled with the notation *re* and *si*.[25] The coordination of the en(thind)$_2$ and en(ind)$_2$ ligands is also chiral and can be labeled with the notation (*R*,*R*) or (*S*,*S*) according to the rules of Chan–Ingold–Prelog[26,27] extended to chiral metallocenes as outlined by Schlögl.[28] The symbols (*R*,*R*) and (*S*,*S*) indicate the absolute configuration of the bridgehead carbon atom of the two ligands. Without loss of generality, all the reported calculations refer to the (*R*,*R*) coordination of the π-ligands.

In order to simplify the description of our calculations and results, the various model sites considered in our work are identified in the following as (olefin)(alkyl)ligand sites. For instance, the notation (*re*-propene)-(isobutyl)en(thind)$_2$Mt identifies a model site containing the en(thind)$_2$ ligand, a propene molecule coordinated *re* to the metal atom (Mt = Zr or Ti), and the (primary) growing chain simulated by an isobutyl group. The geometries of model sites containing the Zr atom and the en(thind)$_2$ ligand have been constructed, as in previous calculations, using internal parameters coincident with those found by Brintzinger and co-workers in the crystalline *rac*-en(thind)$_2$ZrCl$_2$.[29] Test calculations have been performed also considering other conformations of low energy for the six-membered rings, giving substantially analogous results. The geometry of model sites containing Zr and the en(ind)$_2$ ligand, as in previous calculations, has been obtained from the latter by assuming standard geometry for the six-membered aromatic rings. Strictly analogous results have been obtained by fixing the geometry of coordination of the *rac*-en(ind)$_2$ ligand described for the crystalline structures reported in refs 30 and 31.

As in refs 6–9, the geometric parameters relative to the coordinated olefin have been derived from the crystal structure of bis(pentamethylcyclopentadienyl) (ethene)titanium.[16] The distance Zr–C (chain) has been assumed to be 2.28 Å, as observed in some σ-alkyl Zr complexes,[32] while the distance Zr–C (olefin) has been set equal to 2.30 Å, that is, 0.02 Å longer than the distance Zr–C (chain), to be consistent with the analogous distances observed in titanium complexes.[16,33–36] Test calculations have been performed by assuming the bond distance Zr–C (chain) to be equal to 2.25 Å, which is an average of the values observed in cationic zirconocene complexes,[37–44] and/or also assuming the distance Zr–C (olefin) to be equal to 2.36 Å, which is the value observed in the structure of $Cp_2Zr(C_2H_4)(PMe_3)$.[15]

In the case of model sites containing the titanium atom and the en(thind)$_2$ ligand, the geometry of coordination of the ligands has been

(19) Castonguay, L. A.; Rappé, A. K. *J. Am. Chem. Soc.* **1992**, *114*, 5832.
(20) Grassi, A.; Zambelli, A.; Resconi, L.; Albizzati, E.; Mazzocchi, R. *Macromolecules* **1988**, *21*, 617.
(21) Cheng, H. N.; Ewen, J. A. *Makromol. Chem.* **1989**, *190*, 1931.
(22) Soga, K.; Shiono, T.; Takemura, S.; Kaminsky, W. *Makromol. Chem. Rapid Commun.* **1987**, *8*, 305.
(23) Mizuno, A.; Tsutsui, T.; Kashiwa, N. *Polymer* **1992**, *33*, 254.
(24) Busico, V.; Cipullo, R.; Corradini, P. *Makromol. Chem. Rapid Commun.* **1993**, *14*, 97.
(25) Hanson, K. R. *J. Am. Chem. Soc.* **1966**, *88*, 2731.
(26) Chan, R. S.; Ingold, C.; Prelog, V. *Angew. Chem., Int. Ed. Engl.* **1966**, *5*, 385.
(27) Prelog, V.; Helmchem, G. *Angew. Chem., Int. Ed. Engl.* **1982**, *21*, 567.
(28) Schlögl, K. *Top. Stereochem.* **1966**, *1*, 39.
(29) Wild, F. R. W. P.; Wasiucionek, M.; Huttner, G.; Brintzinger, H. H. *J. Organomet. Chem.* **1985**, *288*, 63.
(30) Horton, A. D.; Orpen, A. G. *Organometallics* **1991**, *10*, 3910.
(31) Horton, A. D.; Orpen, A. G. *Organometallics* **1992**, *11*, 1193.
(32) Hunter, W. E.; Hrncir, D. C.; Vann Bynum, R. V.; Penttila, R. A.; Atwood, J. L. *Organometallics* **1983**, *2*, 750.
(33) Davies, G. R.; Jarvis, J. A. J.; Kilbourn, B. T. *J. Chem. Soc., Chem. Commun.* **1971**, 1511.
(34) Bassi, I. W.; Allegra, G.; Scordamaglia, R.; Chioccola, G. *J. Am. Chem. Soc.* **1971**, *93*, 3787.
(35) Dawoodi, Z.; Green, M. L. H.; Mtetwa, V. S. B.; Prout, K. *J. Chem. Soc., Chem. Commun* **1982**, 802.
(36) Dawoodi, Z.; Green, M. L. H.; Mtetwa, V. S. B.; Prout, K. *J. Chem. Soc., Chem. Commun.* **1982**, 1410.
(37) Jordan, R.; Bajgur, C.; Willet, R.; Scott, B. *J. Am. Chem. Soc.* **1986**, *108*, 7410.
(38) Hlatky, G.; Turner, H.; Eckman, R. *J. Am. Chem. Soc.* **1989**, *111*, 2728.
(39) Amorose, D. M.; Lee, R. A.; Petersen, J. L. *Organometallics* **1991**, *10*, 2191.
(40) Horton, A.; Orpen, G. A. *Organometallics* **1991**, *10*, 3910.
(41) Jordan, R. F.; LaPointe, R. E.; Bradley, P. K.; Baezinger, N. C. *Organometallics* **1989**, *8*, 2892.
(42) Jordan, R. F.; Taylor, D. F.; Baezinger, N. C. *Organometallics* **1990**, *9*, 1546.
(43) Jordan, R. F.; Taylor, D. F.; Baezinger, N. C. *Organometallics* **1987**, *6*, 1041.
(44) Jordan, R. F.; Bradley, P. K.; Baezinger, N. C. *J. Am. Chem. Soc.* **1990**, *112*, 1289.

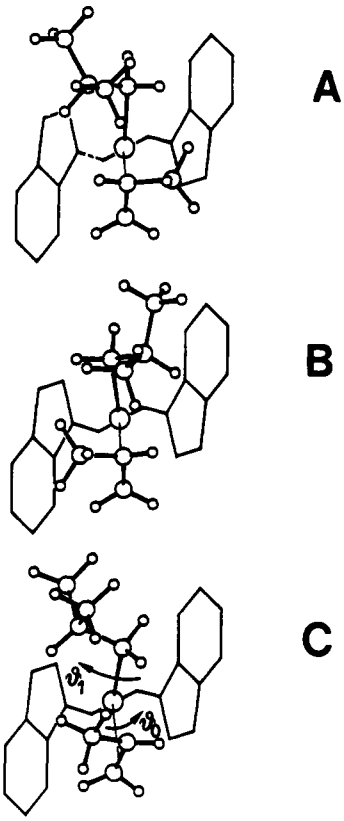

Figure 1. Models for the primary insertion of propene into a primary polypropene growing chain, when the aromatic ligand is en(ind)$_2$. A, B, and C correspond to the minimum energy situations labeled with the letters a, b, and c in Figure 2A. Model A, with *re* propene coordination, is the only one suitable for the insertion (see text). For clarity, only the C–C bonds are sketched for the aromatic ligands.

assumed to be coincident with that found by Brintzinger and co-workers for the *rac*-en(thind)$_2$TiCl$_2$[45] and for the en(thind)$_2$ ligand, while the geometry of model sites containing Ti and the en(ind)$_2$ ligand has been obtained from the latter by assuming standard geometry for the six-membered aromatic rings. The distance Ti–C (olefin) has been set equal to 2.17 Å,[16] while the ditance Ti–C (chain) has been assumed to be equal to 2.15 Å.[33-36]

In all the systems considered here an out-of-plane bending angle of 10° for the H atoms bonded to the aromatic rings has been permitted. Analogous bendings are normally observed for alkyl groups on the π-ligands in metallocenes.[46] Moreover, the assumption of an out-of-plane bending of the H atoms tends to compensate for the rigidity, assumed for the π-ligands.

The main internal coordinates, which have been varied in our calculations (see Figure 1C), are defined as in our previous papers.[6-9] The most important internal coordinates which have been varied are the dihedral angle θ_0 associated with rotations of the olefin around the axis connecting the metal to the center of the double bond and the internal rotation angles θ_1 and θ_2, associated with rotations around the bond between the metal atom and the first carbon atom of the growing chain and around the bond between the first and the second carbon atoms of the growing chain, respectively. At θ_0 near 0° the olefin is oriented in a way suitable for primary insertion, while θ_0 near 180° corresponds to an orientation suitable for secondary insertion. θ_1 near 0° corresponds to the conformation having the first C–C bond of the growing chain eclipsed with respect to the axis connecting the metal atom to the center of the double bond of the olefin. θ_2 = 0° corresponds to the conformation having the Zr–C bond of the growing chain eclipsed with respect to the C–H (C–C) bond on the second carbon atom of the isobutyl (*sec*-butyl) group. The torsional potentials for the rotations θ_0 and θ_1 are not known and therefore are not included in our calculations. While we expect such energy contribution to be small for θ_1, it may not be so for θ_0. Since we are mainly interested in situations with θ_0 not far from 0° (for primary insertion) or not far from 180° (for secondary insertion), the inclusion of such a torsional potential would not change significantly our conclusions. For the rotation θ_2, the torsional potential reported in ref 47 is included.

The bond angles centered on sp^3 carbon atoms have been optimized in each calculation, the bending contribution to the total energy being evaluated according to ref 47. The bending potentials for the Zr–C–C and Zr–C–H angles have been arbitrarily assumed to be equal to the potential for the C–C–C and C–C–H angles, respectively.

At variance with previous calculations,[6-9] in which the two bonds Zr–C (chain) and Zr–(center of the olefin double bond) were confined in the plane defined by the two metal–chlorine bonds in the precursor compounds, the geometry around the metal atoms has been completely relaxed in this work, except for the angle defined by the centers of the two five-membered aromatic rings and by the metal atom. Anyway, as previously, the angle between the center of the double bond of the olefin, the metal atom, and the first carbon atom of the growing chain has been restrained in the experimentally observed range 91–99°.[48,49]

Since the literature values of the bending constants for bond angles centered on metal atoms[50,51] are roughly of the same magnitude as the H–C–H bending constant, we arbitrarily assumed the bending constant for the various X–Mt–X angles to be equal to that for the H–C–H angle. (*X* stands for the center of the five-membered rings, the center of the double bond of the propene, and the first carbon atom of the growing chain.) Moreover, considering the nearly tetrahedral geometry of coordination at the metal atom, the minimum energy X–Mt–X bond angles were assumed to be 109.5°. (It is, however, worth noting that the numerical results are substantially unchanged for minimum energy bond angles in the range 105–110°.)

As described in the following section, this makes all the energy minima broader than in fixed geometry calculations; however, the energy differences between the various low-energy conformations are practically unchanged.

As in our previous papers,[6-9] possible electronic contributions to the energy have not been considered. This approximation is based on the reasonable hypotheses that the differences of electronic energy at the coordination step are obviously negligible for different chiralities of coordination of propene (related to the enantioselectivity) and are quite small for the two different orientations of propene with $\theta_0 \approx 0°$ and $\theta_0 \approx 180°$ (related to the regioselectivity). In principle, electronic contributions could lead to minimum energy geometries at the metal atom significantly different from those evaluated by simple molecular mechanics calculations, thus having an indirect influence on the evaluated energy differences. However, this does not seem to be the case for our models, since the geometry at the metal atom predicted on the sole basis of the nonbonded interactions is very close to that found in similar complexes characterized by X-ray diffraction.[6]

The method of calculation of the nonbonded potential energy has been previously described[52] and is not reported here. The results presented in this paper are obtained with the parameters proposed by Scheraga and co-workers.[53] In order to test the dependence of the results on the particular choice of the parameters in the potential functions, some calculations have been also performed by using the parameters proposed by Flory and co-workers[47,54,55] and/or treating the CH$_2$ and CH$_3$ groups as spherical domains.[54] Although the results are numerically different in the various cases, the overall trends and the locations of the energy minima are nearly the same. As far as the metal atoms are concerned, it has been shown[56-58] for several complexes that the computed conformations of the ligands are practically independent of the nonbonded

(45) Wild, F. R. W. P.; Zsolnai, L.; Huttner, G.; Brintzinger, H. H. *J. Organomet. Chem.* **1982**, *232*, 233.
(46) Wochner, F.; Zsolnai, L.; Huttner, G.; Brintzinger, H. H. *J. Organomet. Chem.* **1985**, *288*, 69.
(47) Suter, U. W.; Flory, P. J. *Macromolecules* **1975**, *8*, 765.
(48) Schafer, A.; Karl, E.; Zsolnai, L.; Huttner, G.; Brintzinger, H. H. *J. Organomet. Chem.* **1987**, *328*, 87.
(49) Cozak, D.; Melnik, M. *Coord. Chem. Rev.* **1986**, *74*, 53.
(50) Hancock, R. D. *Prog. Inorg. Chem.* **1989**, *37*, 187.
(51) Thiem, H. J.; Brandl, M.; Breslow, R. *J. Am. Chem. Soc.* **1988**, *110*, 8612.
(52) Ammendola, P.; Guerra, G.; Villani, V. *Makromol. Chem.* **1984**, *185*, 2599.
(53) Ool, T.; Scott, R. A.; Vandekooi, K.; Scheraga, H. A. *J. Chem. Phys.* **1967**, *46*, 4410.
(54) Sundararajan, P. R.; Flory, P. J. *J. Am. Chem. Soc.* **1974**, *96*, 5025.
(55) Yoon, D. Y.; Sundararajan, P. R.; Flory, P. J. *Macromolecules* **1975**, *8*, 776.
(56) Corradini, P.; Barone, V.; Fusco, R.; Guerra, G. *Eur. Polym. J.* **1979**, *15*, 1133.
(57) Dwyer, M.; Searle, G. A. *J. Chem. Soc., Chem. Commun.* **1972**, 726.
(58) Niketic, S. R.; Rasmussen, K.; Waldluye, F.; Llfson, S. *Acta Chem. Scand.* **1976**, *A30*, 485.

interactions involving the metal atoms. We have verified this conclusion in our case by some test computations with a range of parameters for the potential functions involving the metal atoms (Zr ≡ C, Zr ≡ Cl, Zr neglected). Therefore, our final choice has been to completely neglect the interactions involving the metal atom.

The same zero of energy is adopted in the following for model sites with the same metal atom and the same aromatic ligand, irrespective of the coordination chirality of the propene monomer and of the primary or secondary nature of the growing chain. On the contrary, energy data and plots referring to model sites with different metals and/or with different π-ligands are not on the same energy scale.

Model intermediates corresponding to the coordination stage are considered sufficiently close to the transition state only if the insertion can occur through a process of "least nuclear motion".[59-63] This corresponds to geometries of the catalytic site intermediates for which (i) the double bond of the olefin is nearly parallel to the bond between the metal atom and the growing chain ($\theta_0 \approx 0°$ or $\theta_0 \approx 180°$) and (ii) the first C–C bond of the chain is nearly perpendicular to the plane defined by the double bond of the monomer and by the metal atom ($50° < \theta_1 < 130°$ rather than $\theta_1 \approx 180°$).

Although the energy optimizations are more complete than in previous works, we still believe that the numerical results of our calculations cannot be trusted as such. This is especially true for conformations far from the absolute energy minima, because of the inaptitude of the energy functions in such regions and because of the simplifying assumption of constancy (rather than near-constancy) of several internal coordinates. However, we also believe that the trends suggested by our results are realistic, in the sense that conformations having low energy according to our calculations are not likely to be substantially different from the energy minima of the catalytic system. Furthermore, although the numerical values of the energy differences depend on the exact geometry and on the energy parameters adopted in the calculations, no reasonable adjustment of these parameters seems to be able to modify our conclusions. As far as the results of our calculations are in qualitative, or perhaps semiquantitative, agreement with all the relevant experimental findings, we also believe that such calculations can be used in a predictive way.

Results and Discussion

Insertion of Propene into a Primary Growing Chain. Figure 2, parts A and B, plots, as a function of θ_1, the optimized energy for the catalytic site models (propene)(isobutyl)en(ind)$_2$Zr and (propene)(isobutyl)en(thind)$_2$Zr with (*R*,*R*) chirality of coordination of the aromatic ligands, respectively. The starting point for the energy optimizations in Figure 2 was the conformation with $\theta_0 = 0°$; whatever the energy, the absolute value of θ_0 for the optimized conformations is not higher than 20°. Hence, these models simulate situations suitable for the primary insertion of propene into a primary polypropene growing chain. The full and dashed lines refer to *re*- and *si*-coordinated propene, respectively.

The plots in Figure 2 are in good qualitative agreement with those reported in previous papers (see, for instance, Figure 6 in ref 6 or Figure 5 in ref 10), although the more complete energy optimizations adopted in this work lead to some quantitative differences (in particular, to broader energy minima). As previously described, the enantioselectivity of these models is not due to direct interactions of the aromatic ligands with the monomer but to interactions of the aromatic ligands with the growing chain, determining its chiral orientation ($\theta_1 \approx -60°$ preferred to $\theta_1 \approx +60°$), which, in turn, discriminates between the two prochiral faces of the propene monomer.

Models corresponding to the minimum energy situations labeled with the letters a, b, and c in Figure 2A are sketched in Figure 1, parts A, B, and C, respectively. The models in Figures 1, parts A and B, minimize the interactions between the growing chain (at $\theta_1 \approx -60°$ and at $\theta_1 \approx +60°$) and the methyl of the propene monomer (*re* and *si* coordinated, respectively). Therefore, as

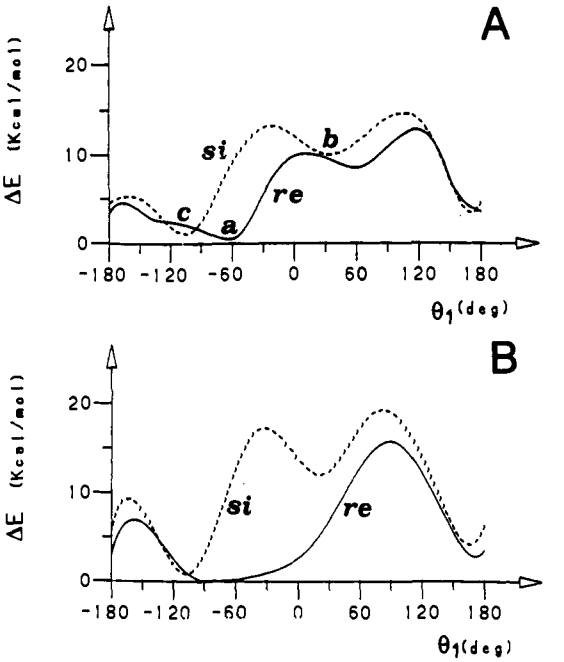

Figure 2. Optimized energy as a function of θ_1, with $\theta_0 \approx 0°$ (see text), for two models of catalytic intermediates with (*R*,*R*) chirality of coordination of the aromatic ligands: (A) (propene)(isobutyl)en(ind)$_2$Zr; (B) (propene)(isobutyl)en(thind)$_2$Zr. These models simulate situations suitable for the primary insertion of propene into a primary polypropene growing chain. The full and dashed lines refer to *re*- and *si*-coordinated propene, respectively. The models corresponding to the energy minima labeled with a, b, and c are sketched in Figure 1.

discussed in previous papers,[1,6,10] they are both assumed to be suitable for the successive insertion reaction. However, the model with *si* monomer coordination (Figure 1B) is strongly disfavored by repulsive interactions of the growing chain at $\theta_1 \approx +60°$ with one of the indenyl groups. The other model with *si* monomer coordination, but with $\theta_1 \approx -60°$ (Figure 1C), is higher in energy (1–2 kcal/mol) with respect to the model with *re* monomer coordination (Figure 1A). Moreover, since the methyl group of the propene and the second carbon atom (and its substituents) of the growing chain are on the same side with respect to the plane defined by the Zr–C bonds, the model of Figure 1C (corresponding to the energy minimum c in Figure 2A) is assumed to be unsuitable for the successive monomer insertion.[1,10]

Figure 3 plots as a function of θ_0 the optimized energies for the two model sites with the en(ind)$_2$ (Figure 3A) and the en(thind)$_2$ (Figure 3B) ligands. For both model sites, the conformations with $\theta_0 \approx 180°$ are of higher energy than those with $\theta_0 \approx 0°$ in the case of *re* monomer coordination. The dashed curves, corresponding to model sites with *si*-coordinated monomer, show broad minima centered at $\theta_0 \approx 150°$. These minima would probably be increased in energy by inclusion of a torsional potential around θ_0. Furthermore, one can reasonably assume that the double bond of the olefin and the Mt–chain bond have to be nearly coplanar in the transition state of the insertion reaction. Hence, in the framework of the assumed mechanism, for these models there is a contribution of the nonbonded interactions in favor of the monomer coordination suitable for (and perhaps relevant to) the primary monomer insertion (of nearly 3 and 5 kcal/mol for the model sites with the en(ind)$_2$ and the en(thind)$_2$ ligands, respectively).

Figure 3 also indicates that the energy of models with *re*-coordinated monomer is always lower than that of models with *si*-coordinated monomer when $\theta_0 \approx 0°$, while the opposite is true when $\theta_0 \approx 180°$. Hence, as previously reported[6] but not explicitly evidenced, model sites with (*R*,*R*) coordination chirality of the aromatic ligand favor the *re* monomer coordination for the orientation suitable for a primary insertion ($\theta_0 \approx 0°$), while they

(59) Cossee, P. *Tetrahedron Lett.* **1960**, *17*, 12; *Ibid.* **1960**, *17*, 17; *J. Catal.* **1964**, *3*, 80; *Ibid.* **1964**, *3*, 99.
(60) Hine, J. *J. Org. Chem.* **1966**, *31*, 1236.
(61) Hine, J. *Adv. Phys. Org. Chem.* **1977**, *15*, 1.
(62) Sinnott, M. L. *Adv. Phys. Org. Chem.* **1988**, *24*, 113.
(63) Venditto, V.; Corradini, P.; Guerra, G.; Fusco, R. *Eur. Polym. J.* **1991**, *27*, 45.

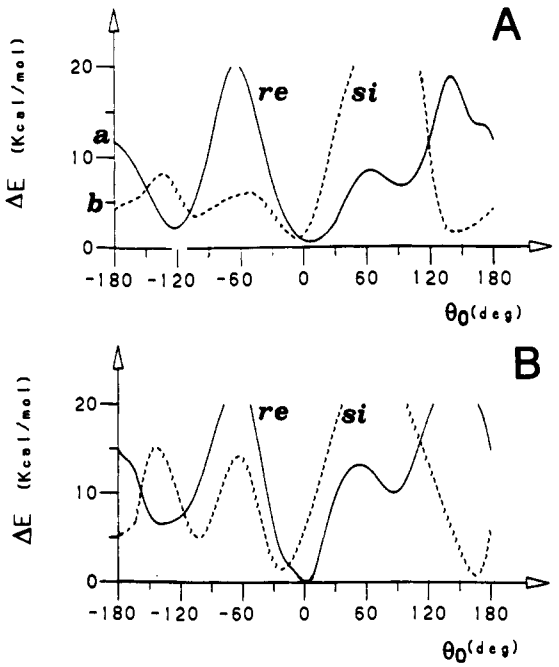

Figure 3. Optimized energy as a function of θ_0 for the models of Figure 1: (A) (propene)(isobutyl)en(ind)$_2$Zr; (B) (propene)(isobutyl)en(thind)$_2$Zr. The full and dashed lines refer to *re*- and *si*-coordinated propene, respectively. The models corresponding to the situations with $\theta_0 \approx 180°$ labeled a and b are sketched in Figure 4, parts A and B, respectively.

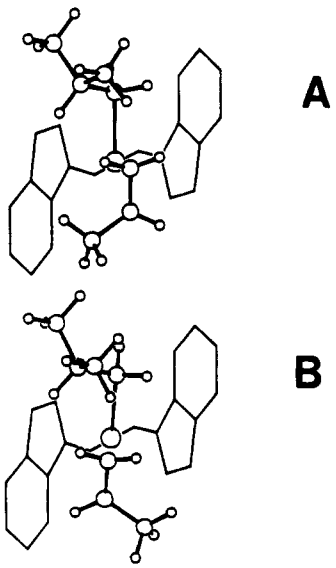

Figure 4. Models for the secondary insertion of propene into a primary polypropene growing chain, when the aromatic ligand is en(ind)$_2$. A and B correspond to the situations labeled with the letters a and b in Figure 3A. Model B, with *si* propene coordination, is the only one suitable for monomer insertion (see text).

favor the *si* monomer coordination for the orientation suitable for a fortuitous secondary insertion ($\theta_0 \approx 180°$).

Models corresponding to the situations with $\theta_0 \approx 180°$, labeled with the letters a and b in Figure 3A, are sketched in Figure 4, parts A and B, respectively. It is apparent, also on inspection, that the preference for the *si* monomer coordination (Figure 4B) is due to lower interactions of the methyl group of the olefin with the aromatic ligands. Hence, contrary to the case of the enantioselectivity for the primary insertion, the enantioselectivity of the models for the secondary insertion of propene is due to direct interactions of the aromatic ligands with the monomer.

Insertion of Propene into a Secondary Growing Chain. Figure 5, parts A and B, plots, as a function of θ_0, the optimized energy

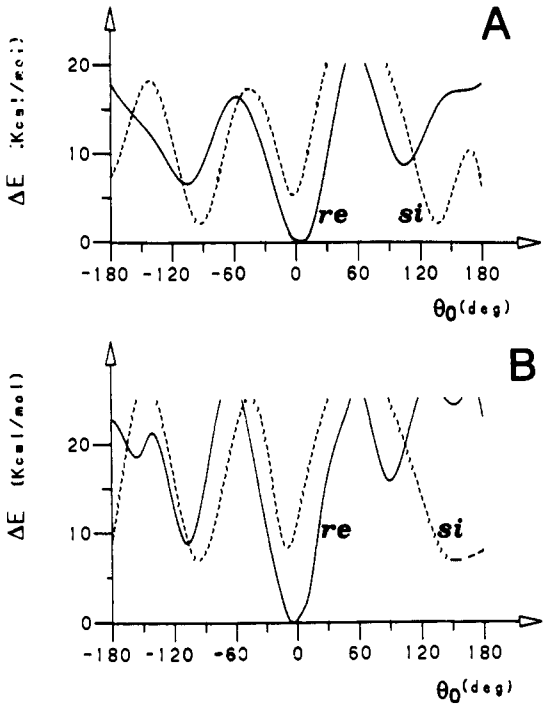

Figure 5. Optimized energy as a function of θ_0 for two models of catalytic intermediates with (*R*,*R*) chirality of coordination of the aromatic ligands: (A) (propene)(*sec*-butyl)en(ind)$_2$Zr; (B) (propene)(*sec*-butyl)-en(thind)$_2$Zr. These models simulate situations suitable for the insertion of propene into a secondary polypropene growing chain. The full and dashed lines refer to *re*- and *si*-coordinated propene, respectively.

for the catalytic site models (propene)(*sec*-butyl)en(ind)$_2$Zr and (propene)(*sec*-butyl)en(thind)$_2$Zr, respectively, with (*R*,*R*) chirality of coordination of the aromatic ligands. These models simulate situations suitable for the insertion of propene into a secondary polypropene growing chain. The full and dashed lines refer, as before, to *re*- and *si*-coordinated propene, respectively.

The plots shown in Figure 5 lead to conclusions analogous to those obtained in Figure 3 (see before). In other words, our calculations indicate that the nonbonded interactions favor the monomer coordination which is suitable for the primary insertion (with $\theta_0 \approx 0°$), with respect to the monomer coordination suitable for the secondary insertion (with $\theta_0 \approx 180°$), independent of the primary or secondary nature of the growing chain.

Figure 6A,B plots the optimized energies of the model sites of Figure 5A,B as a function of θ_1, using $\theta_0 = 0°$ as a starting point. Both plots indicate that the corresponding models are enantioselective in favor of the *re* enantioface of the monomer, as already observed for the models with a primary growing chain (Figure 2). However, the energy difference between the lowest energy conformation observed in Figure 6 for the *si* enantioface of the monomer and that observed for the *re* enantioface (in the ranges of θ_1 suitable for insertion) is much smaller in Figure 6A than in Figure 6B. This suggests a less pronounced enantioselectivity in favour of the *re* enantioface for the model with the en(ind)$_2$ ligand with respect to the corresponding model with the en(thind)$_2$ ligand.

The models corresponding to the minimum energy situations labeled with the letters a and b in Figure 6A are sketched in Figure 7, parts A and B, respectively. As for the models with a primary growing chain shown in Figure 1A,B, the models of Figure 7A,B minimize the interactions between the growing chain and the methyl group of the propene monomer (*re* and *si* coordinated, respectively). Hence, they are both assumed to be suitable for the successive insertion reaction (see before). The model with *si* monomer coordination (Figure 7B) is still disfavored with respect to the model with *re* monomer coordination (Figure 7A). However, with respect to the model with a primary chain (Figure

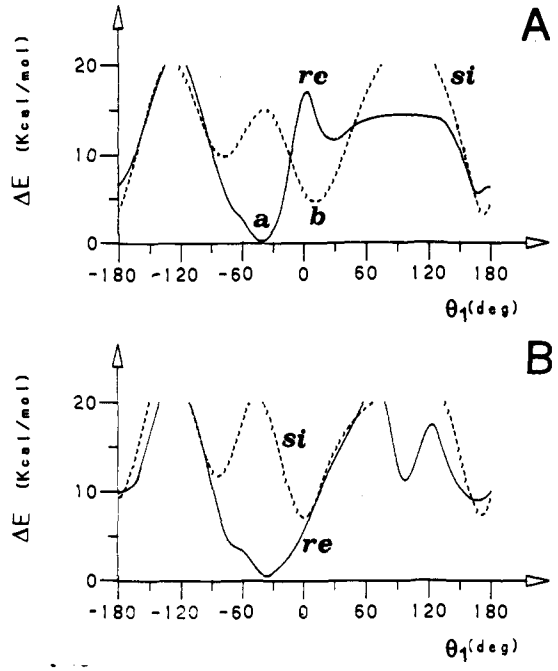

Figure 6. Optimized energy as a function of θ_1, with $\theta_0 \approx 0°$ (see text), for the models of Figure 5: (A) (propene)(*sec*-butyl)en(ind)$_2$Zr; (B) (propene)(*sec*-butyl)en(thind)$_2$Zr. The full and dashed lines refer to *re*- and *si*-coordinated propene, respectively. The models corresponding to the energy minimum situations labeled with a and b are sketched in Figure 7.

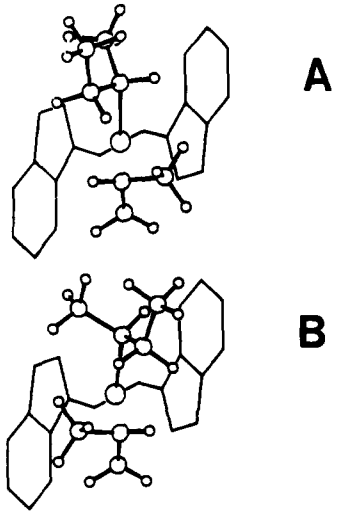

Figure 7. Models for the primary insertion of propene into a secondary polypropene growing chain, when the aromatic ligand is et(ind)$_2$. A and B correspond to the situations labeled with the letters a and b in Figure 6A. Model A, with *re* propene coordination, is favored for the insertion of monomer; model B, however, with *si* propene coordination, is also suitable for insertion (see text).

1B), the repulsive interactions between the indenyl ligands and the growing chain (with $\theta_1 \approx +30°$) are much smaller. In fact, positive values of θ_1 place in proximity of one of the aromatic ligands the second carbon atom of the growing chain, which is secondary in the case of a secondary growing chain (Figure 7B), but is tertiary in the case of a primary growing chain (Figure 1B). Similar conformations, with positive values of θ_1, are of high energy in the presence of the bulkier en(thind)$_2$ ligand, even in the case of a secondary polypropene growing chain (Figure 6B).

Hence, these models allow a simple rationalization for the reduced enantioselectivity observed for catalytic systems based on the en(ind)$_2$ ligand when a secondary, rather than a primary, polypropene chain is present. At the same time the models are able to rationalize the high enantioselectivity of the catalytic

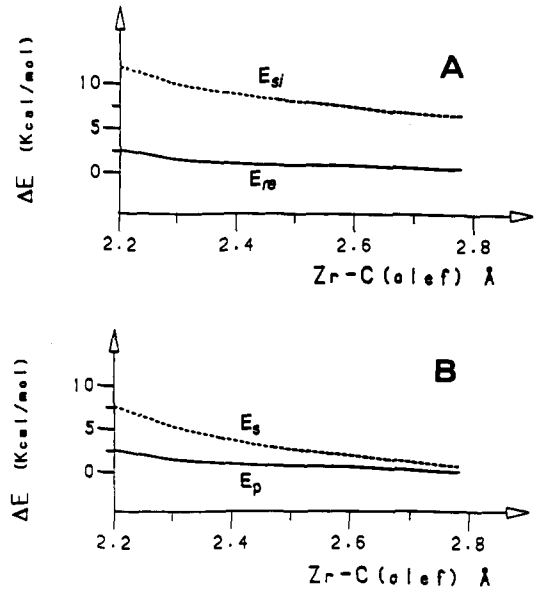

Figure 8. Minimum energy values (E) for the model site (propene)(isobutyl)en(ind)$_2$Zr, as a function of the Zr–C (olefin) distance: (A) E_{si} for the *si* propene coordination with $\theta_0 \approx 0°$, for $\theta_1 \approx +60°$, E_{re} for the *re* propene coordination with $\theta_0 \approx 0°$, for $\theta_1 \approx -60°$; (B) E_p for propene coordination with $\theta_0 \approx 0°$ (suitable for the primary insertion), E_s for propene coordination with $\theta_0 \approx 180°$ (suitable for the secondary insertion).

systems based on the en(thind)$_2$ ligand, independent of the regioregularity of the last inserted monomeric unit.

Dependence of the Calculated Energy Differences on the Zr–C (Olefin) Distance. In the present section the dependence of some of our results on the metal–C (olefin) distance in the coordination intermediates is described. In fact, although we believe that the Zr–C (olefin) distance in the coordination intermediates should be in the range 2.3–2.5 Å, since much larger values have been calculated by the previously cited *ab-initio* studies,[14,18] the dependence of our results on this distance (in the very broad range 2.2–2.8 Å) have been also explored.

As previously discussed, the energy differences between the minima observed for $\theta_0 \approx 0°$ at $\theta_1 \approx +60°$ for *si*-propene (E_{si}) and at $\theta_1 \approx -60°$ for *re*-propene (E_{re}) can be taken, in the framework of our analysis, as an approximation of the energy differences which determine the enantioselectivity. It is worth noting that this kind of evaluation of the enantioselectivity is different from that used by other authors.[14,19,64] In those papers the energy differences between diastereoisomeric situations are evaluated by minimizing the energy in the whole range of θ_1. In our computations we consider only situations suitable for the monomer insertion, and hence, the minimizations with respect to θ_1 are chosen to be only local. This accounts for the much smaller enantioselectivities calculated by other authors.

Values of E_{si} and E_{re} for the primary insertion of propene into a primary growing chain at the model site (propene)(isobutyl)en(ind)$_2$Zr are plotted as a function of the Zr–C (olefin) distance, in Figure 8A. It is apparent that the calculated enantioselectivity ($E_{si} - E_{re}$) is scarcely dependent on the metal–C (olefin) distance, in the range of values considered.

On the other hand, in the framework of our analysis, the energy difference between the minimum energies for $\theta_0 \approx 0°$ (E_p) and $\theta_0 \approx 180°$ (E_s), that is, for propene coordinations suitable for primary and secondary insertions, respectively, can be taken as an indication of a nonbonded energy contribution to the regioselectivity.

The values of E_s and E_p for the propene insertion into a primary growing chain at the model site (propene)(isobutyl)en(ind)$_2$Zr

(64) Hart, J. R.; Rappé, A. K. *J. Am. Chem. Soc.* **1993**, *115*, 6159.

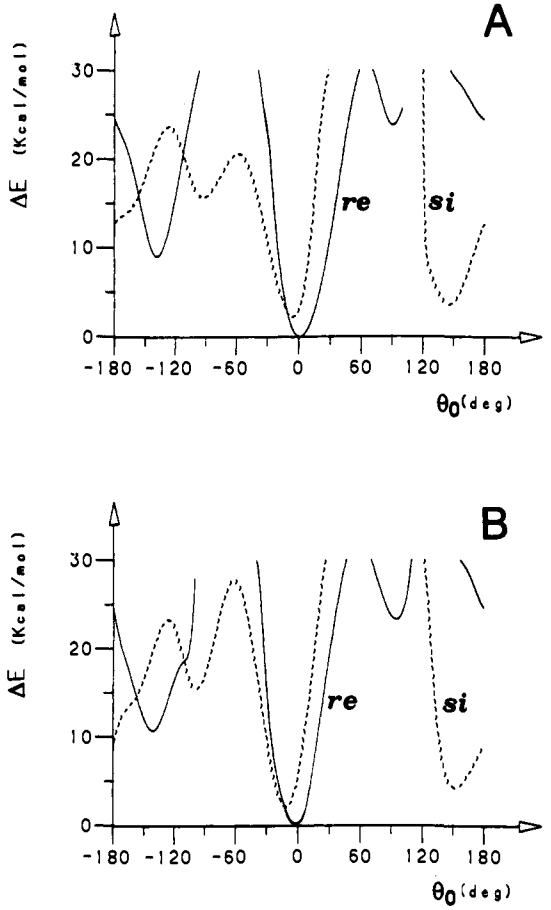

Figure 9. Optimized energy, as a function of θ_0, for two models of catalytic intermediates with (*R*,*R*) chirality of coordination of the aromatic ligands: (A) (propene)(isobutyl)en(ind)$_2$Ti; (B) (propene)(isobutyl)en(thind)$_2$Ti. The only difference with respect to the models in Figure 3 is the nature of the metal (Ti rather than Zr). The full and dashed lines refer to *re*- and *si*-coordinated propene, respectively.

are reported as a function of the Zr–C (olefin) distance in Figure 8B.

It is worth noting that the curves of E_{re} of Figure 8A and of E_p of Figure 8B are coincident. This is due to the fact that the minimum energy values for the primary insertion (optimized with respect to the main internal coordinates) are always obtained for the *re* coordination of propene and for $\theta_1 \approx -60°$. The minimum energy values for the secondary insertion are always obtained for the *si* coordination of propene and for $\theta_1 \approx -60°$. As previously discussed, this corresponds to opposite enantioselectivities of the model intermediates for the primary and secondary insertion of propene.

From a comparison of Figure 8, parts A and B, it is apparent that the nonbonded energy contribution to the regioselectivity is definitely smaller than the nonbonded energy contribution to the enantioselectivity in the whole range, becoming practically negligible for high Zr–C (olefin) distances.

Regiospecificity for Titanium-Based and Zirconium-Based Systems. Indications related to the higher regiospecificity observed for titanocene-based catalytic systems with respect to the corresponding zirconocene-based systems[20] can be obtained on the basis of the nonbonded interactions on similar models of the catalytic sites.

Figure 9, parts A and B, plots, as a function of θ_0, the minimized energy for the catalytic site models (with (*R*,*R*) chirality of coordination of the aromatic ligands) (propene)(isobutyl)en(ind)$_2$Ti and (propene)(isobutyl)en(thind)$_2$Ti, respectively. As in the case of Figure 3, these models simulate situations suitable for the insertion of propene into a primary polypropene growing chain. It is clearly seen that, for both model sites with the en(ind)$_2$ (Figure 9A) and the en(thind)$_2$ (Figure 9B) ligands, the contribution of the nonbonded interactions to the regiospecificity (that is, in the framework of our model, the energy difference between the situations with $\theta_0 \approx 0°$ and $\theta_0 \approx 180°$) is strongly increased with respect to that predicted for the corresponding zirconocene models (Figure 3A,B).

Conclusions

This paper reports the results of detailed molecular mechanics calculations on previously proposed models of catalytic intermediates in the isospecific homogeneous Ziegler–Natta catalysis. It shows that calculations of this kind are able to rationalize the experimental information on the stereochemical configuration of the regioirregular units in isotactic polypropene samples prepared with these catalytic systems. In particular, all the experimental findings listed in the Introduction for polymer samples prepared by catalytic systems based on *rac*-en(thind)$_2$ZrCl$_2$ and *rac*-en(ind)$_2$ZrCl$_2$ are explained by nonbonded interactions active in our models, which we believe to be similar to the transition states for the insertion step.

The enantioselectivity of models for the secondary insertion of monomer (opposite to that of models for the primary insertion) is due to direct interactions of the methyl substituent of the coordinated propene with the π-ligands. We recall, once again, that the enantioselectivity of models for the primary monomer insertion is due instead to the "chiral orientation of the growing chain", that is, to interactions of the methyl substituent of the coordinated propene with the growing chain, whose chiral orientation is determined by nonbonded interactions with the π-ligands.

The experimental finding that the primary insertion of monomer is always favored, even after an occasional secondary insertion, compare well with the observation that in all the considered models, irrespective of the presence of a primary or a secondary growing chain, there is a nonbonded contribution in favor of the monomer coordination suitable for primary insertion ($\theta_0 = 0°$) with respect to the monomer coordination suitable for secondary insertion ($\theta_0 \approx 180°$).

The enantioselectivities observed after an occasional secondary monomer insertion for the two catalytic systems based on the indenyl or on the tetrahydroindenyl ligand, respectively, are easily accounted for in the framework of the mechanism of the "chiral orientation of the growing chain". In fact, substituting the usual primary growing chain with a secondary growing chain reduces the bulkiness of the substituents on the second carbon atom of the chain (which is a secondary carbon for the secondary chain, but is a tertiary carbon for the primary chain). Correspondingly, the energy difference between conformations with positive and negative values of θ_1 (which determines the enantioselectivity of the insertion reaction, in the framework of our model; see before) is reduced in the case of the model with the en(ind)$_2$ ligand, leading to a less pronounced enantioselectivity. The same is not true in the case of models with the bulkier en(thind)$_2$ ligand, for which conformations with positive values of θ_1 are of high energy anyway.

The nonbonded interactions, in models of catalytic intermediates corresponding to the coordination step, are also shown to give a strong contribution to the higher regiospecificity observed for titanocene-based catalysts with respect to zirconocene-based catalysts.

It is worth noting that the proposed models for the catalytic sites (and for the corresponding transition states of the insertion step) in the regioregular (Figure 1A) and regioirregular (Figure 4B) insertion on a primary growing chain are also suitable for the formation of an α-agostic bond between the metal and the hydrogen atom on the opposite side with respect to the incoming

monomer.[37,38,44,65-71] As a matter of fact, the transition state for the insertion step in nonchiral scandium-[72] and chiral zirconium-based[73] catalysts has been found to be α-agostic stabilized.

According to our models the formation of an α-agostic bond may be adjuvant but not crucial for the enantioselectivity of the monomer insertion. In fact, the conformation with $\theta_1 \approx -60°$ (for the complex with the (*R*,*R*) ligand), which discriminates between *si* and *re* monomer insertions, is imposed by the chiral environment even in the absence of a possible α-agostic bond.

Of the two intermediates shown in Figure 7 for the primary insertion on a secondary growing chain, only the one in Figure 7B is suitable for an α-agostic-stabilized monomer insertion. Nevertheless, in the framework of our analysis, the model of Figure 7A would be prevalent for en(ind)$_2$-based catalyst and the only one active for en(thind)$_2$-based catalyst. This indicates that the formation of α-agostic bonds is not necessary to explain the enantioselectivity of the considered catalytic complexes.

Acknowledgment. We thank Dr. E. Albizzati and Dr. L. Resconi of Himont Italia and Prof. A. Zambelli, Dr. P. Longo, and Dr. C. Pellecchia of the University of Salerno for useful discussions. The financial support of the "Progetto Finalizzato Chimica Fine e Secondaria II", of the "Ministero dell'Universitá e della Ricerca Scientifica e Tecnologica" of Italy, and of Montecatini Spherilene is also acknowledged.

(65) Eisch, J. J.; Piotrovsky, A. M.; Brownstein, S. K.; Gabe, E. J.; Lee, F. L. *J. Am. Chem. Soc.* **1985**, *107*, 7219.
(66) Jordan, R. F.; LaPointe, R. E.; Bajgur, C. S.; Echols, S. F.; Willet, R. *J. Am. Chem. Soc.* **1987**, *109*, 4111.
(67) Gassman, P. G.; Callstrom, M. R. *J. Am. Chem. Soc.* **1987**, *109*, 7875.
(68) Bochmann, M.; Wilson, L. M.; Hursthouse, M. B.; Montevalli, M. *Organometallics* **1988**, *7*, 1148.
(69) Burger, B. J.; Thompson, M. E.; Cotter, W. D.; Bercaw, J. E. *J. Am. Chem. Soc.* **1990**, *112*, 1566.
(70) Brookhart, M.; Green, M. L. H.; Wong, L. *Prog. Inorg. Chem.* **1988**, *36*, 1.
(71) Lee, I. M.; Gauthier, W. J.; Ball, J. M.; Iyengar, B.; Collins, S. *Organometallics* **1992**, *11*, 2115.
(72) Kraudelat, H.; Brintzinger, H. H. *Angew. Chem., Int. Ed. Engl.* **1990**, *29*, 1412.
(73) Piers, W. E.; Bercaw, J. E. *J. Am. Chem. Soc.* **1990**, *112*, 9406.